Journal of Inorganic Biochemistry 103 (2009) 288–298

Contents lists available at ScienceDirect

Journal of Inorganic Biochemistry

journal homepage: www.elsevier.com/locate/jinorgbio

# Combined chelation of bi-functional bis-hydroxypiridinone and mono-hydroxypiridinone: Synthesis, solution and *in vivo* evaluation

Sofia Gama [a], Marco Gil [a], Lurdes Gano [b], Etelka Farkas [c], M. Amélia Santos [a,*]

[a] Centro de Química Estrutural, Complexo I, Instituto Superior Técnico, 1049-001 Lisboa, Portugal
[b] Instituto Tecnológico Nuclear, Estrada Nacional no. 10, 2686-953 Sacavém, Portugal
[c] Department of Inorganic and Analytical Chemistry, University of Debrecen, H-4010 Debrecen, Hungary

ARTICLE INFO

*Article history:*
Received 13 August 2008
Received in revised form 22 October 2008
Accepted 28 October 2008
Available online 7 November 2008

*Keywords:*
Combined chelation
Chelation therapy
Hydroxypyridinone
Hydroxypyridinonate complexes
Ternary complex

ABSTRACT

3-Hydroxy-4-pyridinones (3,4-HP) are well known iron-chelators with applications in medicinal chemistry, mainly associated with their high affinity towards trivalent *hard* metal ions (e.g. $M^{3+}$, M = Fe, Al, Ga) and use as decorporating agents in situations of metal accumulation. The polydenticity and the extra-functionality of 3,4-HP derivatives have been explored, aimed at improving the chelating efficacy and the selectivity of the interaction with specific biological receptors. However, the ideal conjugation of both features in one molecular unity usually leads to high molecular weight compounds which can have crossing-membrane limitations.

Herein, a different approach is used combining a arylpiperazine-containing bis-hydroxypyridone ($H_2L^1$) with a biomimetic mono-hydroxypyridinone, ornithine-derivative ($HL^2$), to assess the potential coadjuvating effect that could result from the administration of both compounds for the decorporation of *hard* metal ions. This work reports the results of solution and *in vivo* studies on their chelating efficacy either as a simple binary or a ternary system ($H_2L^1$:$HL^2$:$M^{3+}$), using potentiometric and spectrophotometric methods. The solution complexation studies with Fe(III) indicate that the solubility of the complexes is considerably increased in the ternary system, an important feature for the metal complex excretion, upon the metal sequestration. The results of the *in vivo* studies with $^{67}$Ga-injected mice show differences on the biodistribution profiles of the radiotracer, upon the administration of each chelating agent, that are mainly ascribed to the differences of their extra-functional groups and lipo/hydrophilic character. However, administration of both chelating agents leads to a more steady metal mobilization, which may be attributed to an improved access to different cellular compartments.



## 1. Introduction

Metal ions as iron and aluminium, when in excess or accumulated in tissues, can cause organ dysfunctions and be responsible for serious pathologies or neuropathologies. Hemochromatosis and β-thalassemia (requiring frequent blood transfusions) are examples of iron overload diseases [1,2]. Aluminium accumulation can cause lesions in the central nervous system tissues and be responsible for numerous human neurological disorders [3].

Desferrioxamine (DFO) is a hexadentate tris-hydroxamic siderophore which, for decades, has been used for the excretion of body iron excess. Due to drawbacks associated with DFO, other iron-chelating drugs have been discovered, including 1,2-dimethyl-3-hydroxy-4-pyridinone (commercially available as deferriprone, DFP), an orally active iron-chelating drug also currently used in β-thalassemic patients [4,5]. The combined chelation therapy with DFO and DFP is also being used in special situations of regularly transfused iron-overload patients [6–9], improving the metal mobilization, either in an additive or a synergistic manner, probably through iron "shuttling" from DFP to DFO [10]. The Al-decorporation has also been tested with this and other chelating combinations [11], such as ascorbate (AS) and DFO and/or Feralex-G, (a glycosyl-hydroxypyridinone derivative) [12].

Since the discover of DFP, 3-hydroxy-4-pyridinones (3,4-HP) have been quite explored due to their high affinity towards trivalent *hard* metal ions (M = Fe, Al, Ga). In fact, besides the above referred interest for aluminum and iron chelation, the complexation with gallium is also of interest because gallium radionuclides can be used as imaging diagnosis tools, namely $^{68}$Ga in positron emission tomography (PET) [13,14]. In order to obtain better chelating agents for clinical application, several aspects of the 3,4-HP derivatives

* Corresponding author. Tel.: +351 21 8419000; fax: +351 21 8464455.
*E-mail address:* masantos@mail.ist.utl.pt (M. Amélia Santos).

0162-0134/$ - see front matter © 2008 Elsevier Inc. All rights reserved.
doi:10.1016/j.jinorgbio.2008.10.020

have been explored, namely their polydenticity [15–18] and extrafunctionality [19–21], to improve the chelating efficacy and the selectivity of the biological interaction, respectively. The potential use of 3,4-HPs with complementary properties (e.g. denticity and molecular size) for combined chelation has also been recently analysed [22].

We have developed a new bis-hydroxypyridone extrafunctionalized with an arylpiperazine group, which is known to be recognized by serotonin and sigma receptors, thus providing targeting properties for brain and tumour-imaging agents [23–26]. In this ligand IDAPipPr(3,4-HP)$_2$ ($H_2L^1$), two 3,4-HP chelating moieties are appended to an iminodiacetic acid (IDA) scaffold (see Scheme 1), which has *N*-attached a 1,4-dissubstituted arylpiperazine. However, the saturation of all the $M^{3+}$ six coordination sites by a bis-hydroxypyridinonate ligand can lead to the formation of a dinuclear complex, with expected higher problems on crossing biological membranes than a mononuclear complex. Also, the water solubility is often much lower for a polynuclear than a mononuclear species. Therefore, to overpass these potential limitations of $H_2L^1$ bioavailability and to take profit of eventual coadjuvating effects, the chelating properties of a combination of this bis-hydroxypyridinone ligand with a biomimetic mono-hydroxypyridinone (ornithine-derivative) were also explored.

Herein we report the synthesis of the new tetradentate ligand IDAPipPr(3,4-HP)$_2$ (see Scheme 1), the aqueous solution studies and the *in vivo* assays for metal decorporation. The solution studies allowed the determination of the acid–base properties of this ligand and its chelating ability towards M(III) metal ions (M = Fe, Al, Ga), either alone or combined with the Orn(3,4-HP) chelating agent ($HL^2$). These equilibrium studies were performed using potentiometric and spectrophotometric (UV–Vis, $^1$H NMR) measurements. The lipo/hydrophilic character was also evaluated based on the 1-octanol/water partition coefficient of the compounds.

The *in vivo* biodistribution studies were performed to assess the ability of these chelating systems for the removal of a radiotracer ($^{67}$Ga) injected in mice, as a model of iron-overload animal. The chelating ability of $H_2L^1$ and $HL^2$, when used separately and in combination, were evaluated and compared. Also, the biodistribution of the $^{67}$Ga–$L^1$ complex in different organs was assayed. The results are discussed in comparison with others previously reported for analogous compounds.

## 2. Experimental

### 2.1. Reagents and solutions

All chemicals used were p.a. grade. When anhydrous conditions were necessary, the solvents were dried using methods described in literature [27]. The chemical reactions were followed by TLC. After synthesis and recrystallization of the ligands, the concentrations of their stock solutions were confirmed by the Gran's method [28]. The metal ion (Al, Fe, Ga) stock solutions were prepared, respectively, from $AlCl_3 \cdot 6H_2O$ (in diluted HCl solution), $FeCl_3$ (in diluted HCl solution), $Ga(ClO_4)_3$ (in diluted $HClO_4$ solution).

Except in the case of Ga(III), the concentrations of the metal ion stock solutions were determined gravimetrically via precipitation of quinolin-8-olates. For the measurement of the concentration of Ga(III), known amount of EDTA was added and the excess of EDTA was determined with $ZnCl_2$ stock solution. The HCl concentration of the Fe(III) and Ga(III) solutions were determined by pH-potentiometry.

### 2.2. Synthesis of the ligand

#### 2.2.1. *N-(3-(4-Phenylpiperazin-1-yl)propyl)imino-bis(acetyl(1-(3′-aminopropyl)-3-benzyloxy-2-methyl-4-pyridinone))*

1-(3̀-Aminopropyl)-3-benzyloxy-2-methyl-4-pyridinone hydrochloride [17] (1.004 g, 3.24 mmol) was dissolved in dry methanol (10 mL) cooled in an ice-bath to 0 °C. KOH pellets (397 mg, 7.08 mmol) were added to the cooled solution, under nitrogen. The mixture was stirring for 30 min, the formed KCl was filtered out, the solution was evaporated and the free 1-(3′-aminopropyl)-3-benzyloxy-2-methyl-4-pyridinone was dried under vacuum.

In a different flask, *N*-(3-(4-phenylpiperazin-1-yl)propyl)iminodiacetic acid [29] (625 mg, 1.67 mmol) was dissolved in dry dimethylformamide (DMF, 55 mL). The solution was cooled down in a ice bath, and *N*-methyl-morpholine (0.400 mL, 3.64 mmol) and *O*-benzotriazol-1-yl-*N*,*N*,*N*′,*N*′-tetramethyluronium tetrafluoroborate (TBTU, 1003 mg, 3.12 mmol) were added. The yellow solution obtained was stirred at 0 °C under nitrogen atmosphere for 50 min. The solution was filtered and then added to a solution of free 1-(3′-aminopropyl)-3-benzyloxy-2-methyl-4-pyridinone in dry DMF (*ca.* 6 mL) and cooled down with a NaCl–ice cooling bath.

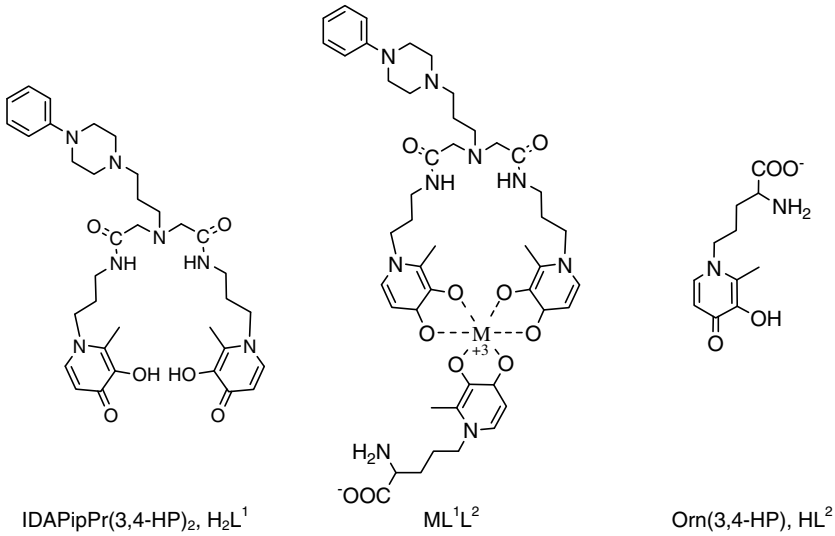


**Scheme 1.**

The reaction mixture was stirred at 0 °C under nitrogen for *ca.* 2 h; the temperature was allowed to increase up to the room temperature it was left stirred during 12 h. After filtered, the solution was evaporated and dried under vacuum. The solid residue was purified by flash chromatography on a silica–gel column, using a mixture of dichloromethane, methanol and ammonia at 1:1:0.005 volume ratio as eluent. Recrystallization with dry MeOH/$CH_3CN$ mixture afforded the pure product as a white solid ($\eta$ = 33%). Mp 89–90 °C, $^1$H NMR ($CDCl_3$/tetramethylsilane, TMS): 8.661 (2H, d), 7.314 (2H + 10H, m), 6.878 (3H, d), 6.235 (2H, d), 5.086 (4H, s), 3.800 (4H, t), 3.201 (8H, m), 3.137 (4H, s), 2.564 (6H, m), 2.375 (2H, t), 2.068 (6H, s), 1.822 (4H, t), 1.678 (2H, t). The splitting of proton resonances in the reported $^1$H NMR spectra are defined as s = singlet, d = doublet, t = triplet, and m = multiplet. *m/z* (fast atom bombardment mass spectra, FAB-MS): 817 (M+1).

#### 2.2.2. N-(3-(4-Phenylpiperazin-1-yl)propyl)imino-bis(acetyl(1-(3′-aminopropyl)-3-hydroxy-2-methyl-4-pyridinone)) (IDAPipPr(3,4-HP)$_2$)

*N*-(3-(4-Phenylpiperazin-1-yl)propyl)imino-bis(acetyl(1-(3′-aminopropyl)-3-benzyloxy-2-methyl-4-pyridinone)) (400 mg, 0.49 mmol) were dissolved in dry methanol (*ca.* 10 mL). To this solution, 10% Pd/C (135 mg) was added and the mixture was stirred at room temperature, during 4 h under $H_2$ (2 atm). After filtration, the solvent was evaporated under vacuum. A white solid was obtained from the recrystallization of the solid residue with dry methanol/ether ($\eta$ = 97%). Mp 112–114 °C, $^1$H NMR ($D_2O$): 7.613 (2H, d), 7.383 (2H, t), 7.101 (3H, d), 6.480 (2H, d), 4.107 (4H, t), 3.327 (4H, t), 3.233 (4H, s), 3.041 (4H, t), 2.841 (2H, t), 2.611 (2H, t), 2.390 (6H, s), 2.010 (4H, t), 1.784 (2H, t). IR (KBr): 3402 cm$^{-1}$ (O–H), 1655 cm$^{-1}$ (C=O), 1561 cm$^{-1}$ (C=C), 1508 cm$^{-1}$ (C=O), 1250 cm$^{-1}$ (C–O). *m/z* (FAB-MS): 665 (M+1). Anal. Calc. to $C_{35}N_7H_{47}O_6K_2{\cdot}H_2O$: C, 55.46; H, 6.52; N, 12.93. Determ.: C, 55.4; H, 6.4; N, 12.6%.

### 2.3. Potentiometric studies

The exact concentration of the carbonate-free KOH titrant was determined by pH-potentiometry. Potentiometric titrations were performed in the pH range 2.0–11.5 or until precipitation. 3 mL samples were used, at 0.2 M KCl ionic strength and 25.0 ± 0.1 °C. During the titrations, oxygen-free argon was continuously bubbled above the samples. Samples were always freshly prepared. In the case of the binary system metal and $H_2L^1$, the ligand concentration was $2.64 \times 10^{-3}$ M and the metal-to-ligand ratios were 1:2 and 1:1. In the studies of the binary system with $H_2L^1$ or $HL^2$, the concentrations were varied in the range $1.5 \times 10^{-3}$–$3 \times 10^{-3}$ M for the ligand $H_2L^1$ and the $H_2L^1$/$HL^2$ molar ratios were 1:1 and 1:2. In the ternary system (metal, $H_2L^1$, $HL^2$) the concentrations were varied in the range $0.5 \times 10^{-3}$–$1 \times 10^{-3}$ M for $H_2L^1$, and the metal-to-$H_2L^1$-to-$HL^2$ ratios were in the range of 1:0.5:2, 1:1:2 and 1:1:1. Potentiometric titrations were carried out with a MOLSPIN pH-meter equipped with a Metrohm 6.0234.100 combined electrode. The titrant was added from a Mol–AcS microburette. The electrode system was calibrated by the method of Irving et al. [30] so that the pH-meter readings could be converted into hydrogen ion concentration. The water ionization constant ($pK_w$) obtained was 13.75 ± 0.01.

The potentiometric measurements were used to find the stoichiometry of species formed in solution and to calculate the corresponding stability constants. In the equilibrium model the metal-hydroxo complexes were included as well as their formation constants reported in literature (Fe(III) [31], Ga(III) [32] and Al(III) [33]). For data fitting analysis, the PSEQUAD computer program [34] was used. These calculations included only the experimental and results obtained before precipitation.

### 2.4. Spectrophotometric studies

UV–Vis measurements were performed for the ligands $H_2L^1$ and $HL^2$ as well as the corresponding Fe(III) and Ga(III) containing systems. The spectra were recorded using a HP 8453 spectrophotometer equipped with 1.000 ± 0.001 cm matched quartz cells at 25.0 °C. For free ligand measurements, *ca.* $6.5 \times 10^{-5}$ M concentrations were used. In the binary system metal-to-ligand ($H_2L^1$), molar ratios range from 1:1 to 1:2, for $C_{Fe} = 2.2 \times 10^{-4}$ M and $C_{Ga}$ = 3–$6 \times 10^{-5}$ M. In the pH range from 0.8 to 2.0, the batch technique was used. It means that the measurements were carried out on individual samples in which the amount of KCl for 0.2 M ionic strength ($I$) was partially or completely replaced by HCl. Therefore the samples were prepared changing the amount of HCl, KCl and $H_2O$ to obtain the intended pH and 0.2 M ionic strength in a 2.5 mL total volume. In the case of the ternary system, only the Fe(III) containing system was measured on a 3 mL sample with $C_{Fe} = 2.01 \times 10^{-4}$ M at 1:1:1 metal-to-$H_2L^1$-to-$HL^2$ stoichiometric conditions.

### 2.5. Partition coefficients

The "shakeflask" method was used to determine the partition coefficient of the ligand in octanol/water (solution TRIS buffered at pH 7.4) at 25 °C, as described in the literature [35]. Partition coefficient represents the ratio of the ligand concentration in the organic phase to that in the aqueous phase. The concentrations in each phase were measured by UV spectrophotometry, using the benzenoid bands ($\pi$–$\pi^*$ transitions at 280 nm) of the ligands.

### 2.6. NMR measurements

A Varian Unity 300 spectrometer was used for the $^1$H NMR measurements. Sodium 3-(trimethylsilyl)-[2,2,3,3-D4]propionate (DSS) was used as internal reference ($\delta$ = 0 ppm) in $D_2O$ samples and TMS in $CDCl_3$ samples, to measure the chemical shifts ($\delta$/ppm). In case of $^1$H NMR titrations, the pD of the samples was measured with a Mettler Toledo U402-M3-S7/200 micro-electrode connected to a Thermo Orion 420 A$^+$ pH meter. The pD values were determined from the equation pD = pH$^*$ + 0.40 [36].

### 2.7. Other measurements

A Leica Galen III hot stage apparatus was used to measure melting points. The solid state IR spectra (KBr pellets) were recorded in a Bio-Rad Merlin, FTS 3000 MX FTIR spectrometer. The mass spectra were carried out in a VG TRIO-2000 GC/MS instrument and the elemental analyses were obtained in a Fisons EA1108 CHNF/O instrument.

### 2.8. In vivo assays

The $^{67}$Ga-citrate injection solution was prepared by diluting $^{67}$Ga-citrate (Ga-67-MM-1; CIS Bio International, Gif–sur–Yvette, France) with saline solution to obtain a final radioactive concentration of 5–10 MBq/100 μL. Animal experiments were carried out in five separate groups of 3–5 female mice CD-1 (randomly bred Charles River, from Barcelona, Spain), weighing approximately 25 g. The animals were intravenously injected with 100 μL (5–10 MBq) of $^{67}$Ga-citrate via the tail vein. Afterwards, they were immediately injected via intraperitoneal, as: (1) single injection with 0.5 μmol of one ligand, IDAPipPr(3,4-HP)$_2$ ($H_2L^1$) or Orn(3,4-HP) ($HL^2$), in 100 μL saline solution; (2) combination of two separate injections of $H_2L^1$ and $HL^2$ saline solutions, the molar ratio $H_2L^1$/$HL^2$ being 1:1, 1:10, 1:100 and 1:1000, respectively, but the final concentration of both ligands was 0.5 μmol in 100 μL. After administration of the ligands, the mice were maintained on a

normal diet *ad libitum*. At 1 h and 24 h post-administration, the animals were killed by cervical dislocation. The radioactive administered dosage and the radioactivity in the sacrificed animals were determined by a dose calibrator (Curiemeter IGC-3; Aloka, Tokyo, Japan). The difference between the radioactivity in the injected and sacrificed animal was assumed to be due to excretion. Tissue samples of main organs were then removed for counting in a gamma counter (Bertyhold LB2111; Berthold Technologies, Bad Wildbad, Germany). Biodistribution results were expressed as percent of injected dose per total organ (%ID/organ) and compared with the previously reported biodistribution profile of $^{67}$Ga citrate. For blood, bone and muscle, total activity was calculated assuming that these organs constitute 7%, 10% and 40% of the total weight, respectively.

## 3. Results and discussion

### 3.1. Synthesis of the ligand IDAPipPr(3,4-HP)$_2$

The method used for the synthesis of the ligand IDAPipPr(3,4-HP)$_2$, *N*-(3-(4-phenylpiperazin-1-yl)propyl)imino-bis(acetyl(1-(3-aminopropyl)-3-hydroxy-2-methyl-4-pyridinone)), is represented in Scheme 2. It involves standard methods with three main steps. Firstly, the arylpiperazine was *N*-attached to the amine group of the backbone, the iminodiacetic acid; then, the *O*-protected hydroxypyridinone arms were coupled to the carboxylic groups of the backbone; the final step was the *O*-deprotection of the hydroxypyridinone. The synthesis of the mono-hydroxypyridinone ornithine-derivative, 1-(4,4-aminocarboxyl-butyl)-3-hydroxy-2-methyl-pyridin-4-one, Orn(3,4-HP) (HL$^2$), was performed according to previously described [20].

### 3.2. Acid–base properties of the ligand IDAPipPr(3,4-HP)$_2$

In its neutral form, the ligand $H_2L^1$ has two dissociable protons, which correspond to the pyridinone hydroxyl groups. HCl excess was added to the sample solution to obtain the fully protonated form of the ligand, with four extra protons in the *N* atoms: two in the two pyridinone-*N* atoms, one in the imino group of the backbone and another one in the piperazine (the remaining piperazine ammonium proton is too acidic most probably due to a H-bond interaction).

Analysis of the potentiometric experimental data, aided by the SUPERQUAD program [37], enabled the calculation of the overall protonation constants ($\log\beta$) from which the values of the stepwise protonation constants ($\log K$) were obtained (see Table 1, which includes all the stepwise protonation constants and stability constants for all the metal-ligand system in study and others reported in literature [38–43], as detaily described and below).

Since the constants calculated from pH-potentiometric data are macroconstants, they cannot be attributed to individual protonating groups, and so the attribution of the stepwise constants of IDAPipPr(3,4-HP)$_2$ was aided by $^1$H NMR titration and analysis of the chemical shift changes with the pH, as shown in Fig. 1.

Although overlapping of the various protonation/deprotonation processes occur, from analysis of the chemical shift profiles along the $^1$H NMR titration and its comparison with the chemical shifts of some model molecules, the following protonation sequence can be assumed: the first higher values ($\log K$ = 10.03 and 9.39) are attributed to the protonation of the hydroxyl oxygens, and they are in agreement with the first $\log K$ of the DMHP (Table 1). Both constants present very similar values due to the symmetry of the molecular structure and independency of the protonation processes. In the $^1$H NMR titration curves, this process is illustrated by the deviation to lower chemical shift of the peaks corresponding to the aromatic hydroxypyridinone protons (peaks 11 and 13). Concerning the third protonation constant ($\log K_3$ = 7.39), comparison between this value and the corresponding one for PipPr(3,4-HP) ($\log K_2$ = 6.68) [44] suggests that this constant should be ascribed to the protonation of the piperazine nitrogen. Analysis of the titration curve profiles corresponding to the chemical shift changes of the peaks 6 and 4 of the ligand molecule, evidences parallel upfield/downfield shifts, followed by reverse downfield/upfield shifts, thus suggesting the existence of a simultaneous competitive deprotonation/protonation process of the two nitrogen atoms of the piperazine ring, with a proton transfer between these two atoms [44]. The monoprotonated form of the piperazine ring may be stabilized from a chair-to-boat conformation change (Scheme 3).

The following two $\log K$ values (3.74 and 3.01) correspond to the protonation of both pyridinyl nitrogens, as evidenced by the change of the chemical shift of proton 10, the aromatic hydroxypyridinone protons (11 and 13) as well as a small shift in the singlet corresponding to the pyridinone-methyl protons (peak 3). The pro-

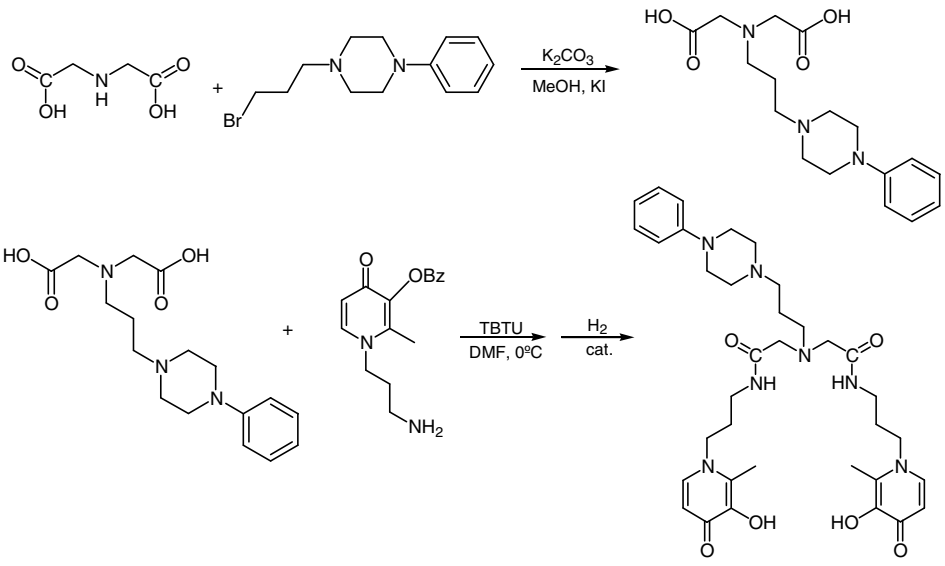


**Scheme 2.**

**Table 1**
Stepwise protonation constants ($\log K_i$) and partition coefficients ($\log P$) at pH = 7.4 for IDAPipPr(3,4-HP)$_2$, Orn(3,4-HP), IDA(3,4-HP)$_2$, 3,4-DMHP ligands and ternary system, as well as the global formation constants ($\log \beta$) for their metal(III) complexes (M = Fe, Ga, Al), at $I$ = 0.2 M KCl and $T$ = 25.0 ± 0.1 °C; pM[a] values for these compounds and some other relevant synthetic and biological ligands.

| Ligands (binary system) | Log $K_i$ | Complex $M_pH_qL_r$ ($p,q,r$) | Log $\beta$ | | | Log $P$ |
|---|---|---|---|---|---|---|
| | | | $Fe_pH_qL_r$ | $Ga_pH_qL_r$ | $Al_pH_qL_r$ | |
| 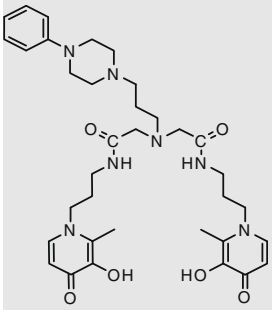 | | (2,−2,2) | – | – | 30.6(4) | −0.31 |
| | | (2,3,3) | 94.59(6) | *ca.* 89.0(1) | 79.6(1) | |
| | | (2,2,3) | – | – | 73.6(5) | |
| | 10.03(1) | (2,1,3) | – | – | 66.3(9) | |
| | 9.39(1) | (2,0,3) | – | *ca.* 74 | 59.4(4) | |
| | 7.39(1) | (1,4,1) | 37.79(1) | – | – | |
| | 3.74(2) | (1,3,1) | 35.88(4) | *ca.* 35.4(2) | 31.77(7) | |
| | 3.01(2) | (1,2,1) | – | – | 29.25(8) | |
| | 2.38(2) | (1,1,1) | 32.51(9) | *ca.* 29.8(3) | 26.64(4) | |
| | | (1,0,1) | 29.69(6)[b] | – | 20.9(4) | |
| | | pM | 25.7[c] | – | 18.0 | |
| IDAPipPr(3,4-HP)$_2$ ($H_2L^1$) | | | | | | |
| 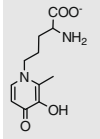 | | (1,1,1) | 25.01 | 23.72 | 21.12 | < −2.00 |
| | | (1,2,2) | 46.20 | 44.86 | 41.10 | |
| | 9.85 | (1,3,3) | 65.68 | 64.46 | 59.64 | |
| | 9.01 | (1,2,3) | 57.72 | 55.93 | 51.09 | |
| | 3.83 | (1,1,3) | 48.43 | 46.46 | 41.74 | |
| | 1.35 | (1,0,3) | 39.42 | 37.32 | 32.36 | |
| | | pM | 21.9 | 20.6 | 15.8 | |
| Orn(3,4-HP)[d] ($HL^2$) | | | | | | |
| 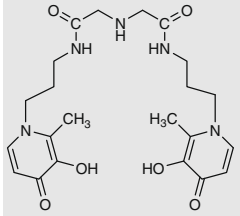 | | (2,−2,2) | 44.00 | – | 32.05 | −1.72 |
| | | (1,−1,1) | – | 18.23 | – | |
| | | (2,3,3) | 89.53 | 84.97 | 76.64 | |
| | 9.94 | (2,2,3) | 85.54 | 80.16 | 71.72 | |
| | 9.44 | (2,1,3) | 79.90 | 74.64 | 66.21 | |
| | 5.42 | (2,0,3) | 74.26 | 68.44 | 60.18 | |
| | 3.54 | (1,3,1) | 33.59 | 33.21 | 30.44 | |
| | 3.11 | (1,2,1) | – | – | 27.71 | |
| | | (1,1,1) | 31.16 | 28.83 | 25.37 | |
| | | (1,0,1) | 26.16 | 24.30 | 20.35 | |
| | | pM | 25.8 | 22.9 | 18.8 | |
| IDAPr(3,4-HP)2[e] | | | | | | |
| 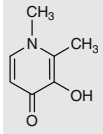 | | (1,0,1) | 15.10 | 13.17 | 12.20 | −1.03 |
| | 9.77 | (1,0,2) | 26.61 | 25.43 | 23.25 | |
| | 3.68 | (1,0,3) | 35.88 | 35.76 | 32.62 | |
| | | pM | 19.3 | 19.4 | 16.1 | |
| 3,4-DMHP[f] | | | | | | |
| DTPA[g] | | pM | 24.6 | 20.9 | 15.2 | <−2 |
| DOTA[g] | | pM | 24.3 | 18.8 | 13.2 | <−2 |
| Desferrioxamine (DFO)[h,i] | | pM | 26.5 | 22.4 | 19.3 | −2 |
| Transferrin | | pM | 20.3[j] | 20.3[k] | 14.5[l] | – |
| Ternary system | | $M_pH_qL^1_rL^2_s$ ($p,q,r,s$) | $Fe_pH_qL^1_rL^2_s$ | $Ga_pH_qL^1_rL^2_s$ | $Al_pH_qL^1_rL^2_s$ | |
| ($L^1$:$L^2$:$M^{3+}$) | – | (1,3,1,1) | 56.81(8) | – | – | – |
| | | (1,2,1,1) | 54.30(7) | – | 46.37(9) | – |
| | | pM | 26.5 | | 17.9 | – |

[a] pM = −log[M] with $C_L/C_M$ = 10 and $C_M = 10^{-6}$ M; ($p,q,r$) means a species with stoichiometry $M_pH_qL_r$;
[b] In this system, this species is not a ML species but probably a protonated mixed hydroxo-species MHL(OH).
[c] This pFe was calculated from extrapolation of the system to pH 7.4, admitting there was no precipitation at that pH value.
[d] Ref. [20].
[e] Ref. [17].
[f] Ref. [39].
[g] Ref. [40].
[h] Ref. [41].
[i] Ref. [4].
[j] Ref. [41].
[k] Ref. [42].
[l] Ref. [43].

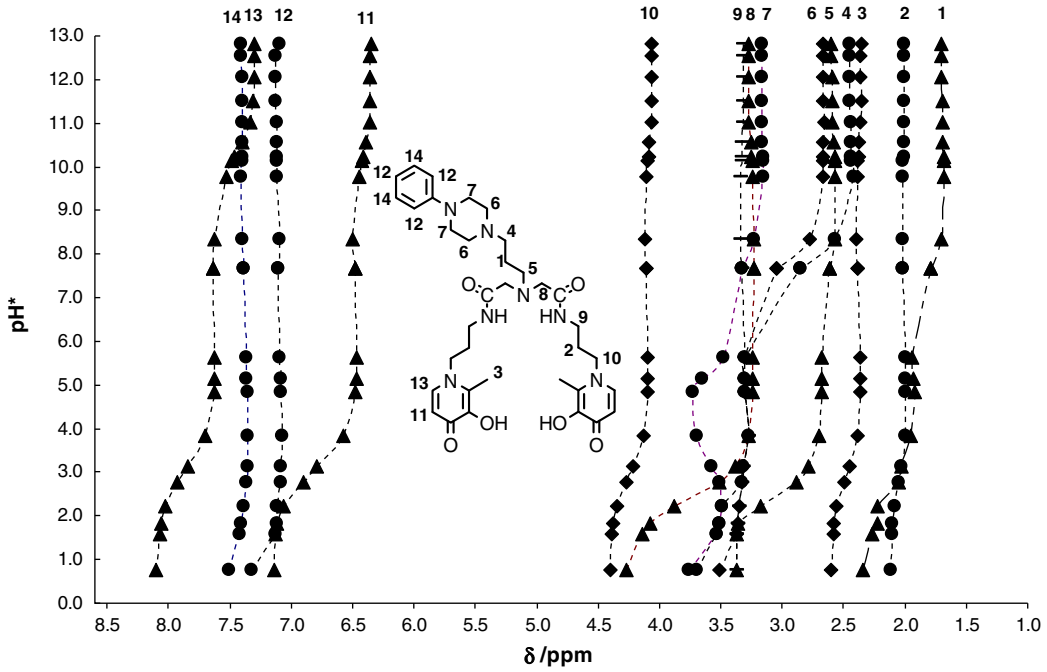


**Fig. 1.** Graphical representation of the chemical shift vs pH* from the $^1$H NMR titration of the free ligand IDAPipPr(3,4-HP)$_2$.

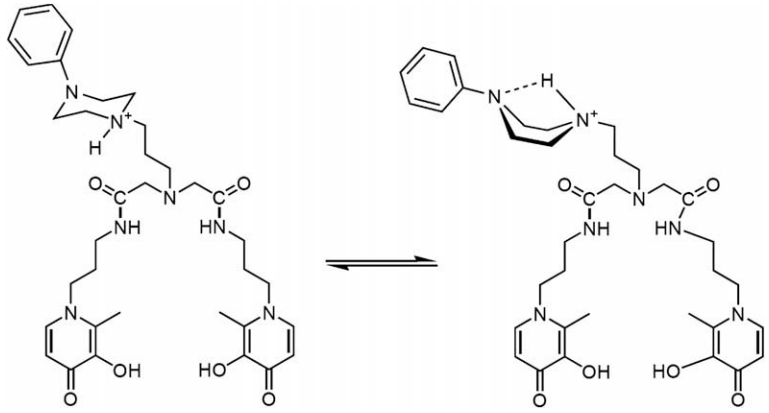

**Scheme 3.**

tonation of the iminodiacetyl tertiary amine is accompanied by a change on chemical shift of the protons corresponding to peaks 8 and 5, which occurs at pH around 2. Therefore, log$K$ = 2.38 can be attributed to the protonation of the tertiary amine. Noteworthy is the decrease of this constant, as compared with the corresponding value (5.42) previously obtained for the *N*-unsubstituted analogue, IDAPr(3,4-HP)$_2$ (Table 1) [17].

The *N*-substituent has also a considerable effect on the lipo/hydrophilic character of these IDA-derivatives; the arylpiperazine derivative is less hydrophilic than the unsubstituted analogue (see Table 1, which also includes the log$P$ values reported for other related compounds (e.g. 3,4-DMHP [39]).

### 3.3. Metal complexation of IDAPipPr(3,4-HP)$_2$

The studies of the complexation of IDAPipPr(3,4-HP)$_2$ with the $M^{3+}$ *hard* metal ions in aqueous solution were firstly performed by potentiometry. However, the very low water solubility of the formed complexes disabled the use of pH-potentiometric measurements for the study of the Fe(III)- and Ga(III)-containing systems. In the case of the Al(III)–ligand system, pH-potentiometric measurements could be used because the precipitation occurs only at pH > 7 (Fig. S1). The fitting analysis of the experimental data, obtained before the precipitation, lead to the equilibrium model which stability constants are presented in Table 1.

Because of the high molar absorptivity associated to the charge transfer band of the Fe(III)–hydroxypyridinonate complexes, *ca.* 10-fold lower concentration could be used in spectrophotometric titrations compared with the pH-metry. In the case of the IDAPipPr(3,4-HP)$_2$/Fe(III) system, for samples with $2 \times 10^{-4}$ M total concentration of metal ion and at 1:1 and 2:1 ligand-to-metal molar ratios (Fig. 2), precipitation occurs at pH around 5, allowing the spectrophotometric register of the charge transfer band up to this pH. Because the complex formation starts at pH < 2, spectra were recorded also at lower pH (Fig. S2), using the batch technique (see Section 2 for the details).

In the case of Ga(III), no characteristic band belongs to the complexes formed. However, using the highly intense UV-band of the ligand, the effect of the Ga(III) on the ligand band in the whole

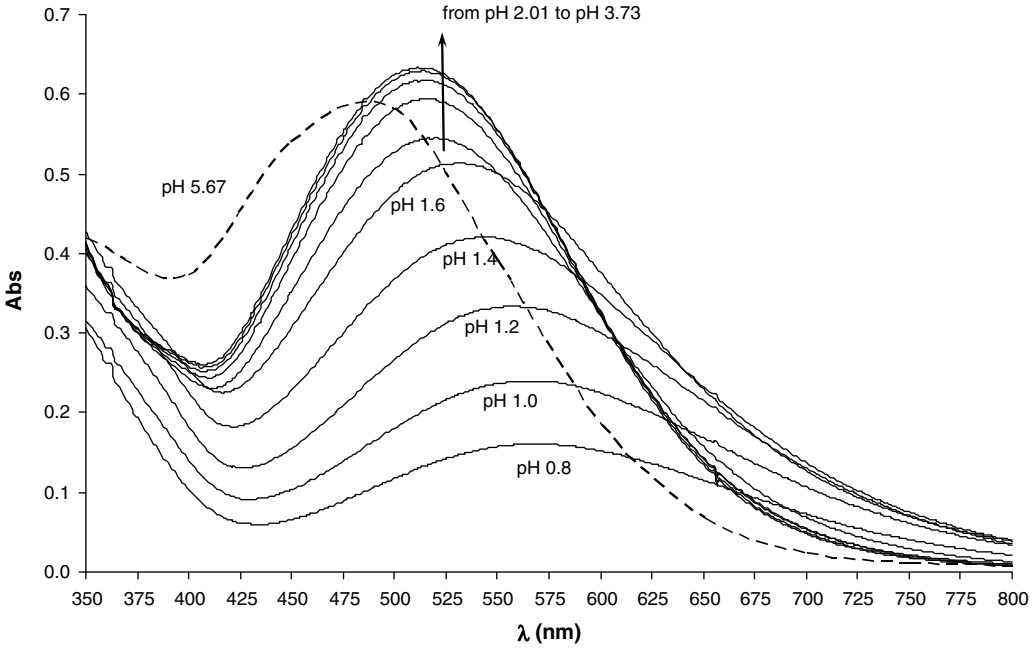


**Fig. 2.** Absorption spectra for the IDAPipPr(3,4-HP)$_2$/Fe(III) system registered at various pH values. $C_L = 2.09 \times 10^{-4}$ M, $C_{Fe} = 2.02 \times 10^{-4}$ M. $T = 25.0$ °C. $I = 0.2$ M KCl, HCl.

measurable pH-ranged could be recorded spectrophotometrically (concentration 100 times lower than that allowed in pH-metry). Therefore, the ligand spectra changes due to its interaction with Ga(III) could be measured as an indirect effect (Fig. S3).

Analysing the above detailed experimental data, the following results were obtained for the metal complexes:

In the case of the Al(III)–containing system, analysis of the titration curves, obtained in the absence and in the presence of Al(III), showed that for this system the complex formation starts at pH around 2–2.5 (see Fig. S1). The first buffered region ends at pH *ca.* 4 (at 4 and 5 base equivalents for 2:1 and 1:1 ligand-to-metal ion molar ratios, respectively, as results of the deprotonation of the three more acidic groups, plus the displacement of two protons per metal ion), then the pH sharply increases. The new buffered region, starting at *ca.* pH 6, can be assigned to the deprotonation of the non-coordinating piperazine nitrogen. This finding suggests that the complexation (which is completed by pH *ca.* 4) occurs via the two hydroxyl-pyridinonate groups. This suggestion is also supported by the fact that the best fit of the titration curves was obtained with the same equilibrium model as that for Al(III)-IDAPr(3,4-HP)$_2$. The corresponding stability constants are also close to each other (Table 1).

For the Fe(III) system, the spectrofotometric data obtained at 1:1 stoichiometric conditions shows a shift of the $\lambda_{max}$ from 560 nm (pH 0.8) to 510 nm (pH 3.7) (see Fig. S2). The later $\lambda_{max}$ and $\varepsilon \cong 3200\ M^{-1}\ cm^{-1}$ are typical spectral parameters for bis-chelated iron-hydroxypyridinonates (the metal ion is coordinationed with two hydroxypyridinonate groups) [38], with its maximum concentration *ca.* pH 3.7. Under ligand excess conditions, the coordination sphere can be completed and this can occur with the formation of dinuclear species, $Fe_2H_xL_3$ ($x = 0, 1, 2, 3$, depending on the protonation state of the non-coordinated *N*-piperazine), as indicated by the blue shift in the $\lambda_{max}$ (from 510 nm at pH 1.8 to 460 nm at pH 5). However, the molar absorptivity ($\varepsilon \cong 4300\ M^{-1}\ cm^{-1}$) is somewhat lower than the characteristic value expected for tris-chelated species ($\varepsilon \cong 5800\ M^{-1}\ cm^{-1}$) [38], which might be caused by the appearance of some precipitate, as also suggested by the increased baseline (Fig. 2). This precipitation might be also responsible for the fact that the stability constants could not be calculated for the dinuclear species involving the deprotonated piperazine-amine group (Table 1).

To evaluate the spectrophotometric results obtained for the Ga(III) system, the free ligand spectra was firstly analysed (Fig. S3a). The fully protonated form of IDAPipPr(3,4-HP)$_2$ has a characteristic band with $\lambda_{max}$ at 276 nm and $\varepsilon \cong 18{,}000\ M^{-1}\ cm^{-1}$, while the corresponding values for the totally deprotonated form are 310 nm and *ca.* $20{,}000\ M^{-1}\ cm^{-1}$, respectively. The spectral band observed at pH 4.8 with $\lambda_{max}$ at 280 nm and $\varepsilon \cong 25{,}000\ M^{-1}\ cm^{-1}$ can be ascribed to the $H_3L^+$ species that starts to be red-shifted (to higher wavelength) with the deprotonation of the hydroxyl pyridinone groups.

Comparative analysis of the spectra obtained for the IDA-PipPr(3,4-HP)$_2$/Ga(III) system and the free ligand (Fig. S3) showed significant effect of the Ga(III) on the ligand spectra obtained in the range of pH 1.2–8. Although the spectra could be registered, the calculation of the stability constants for the complexes was precluded. Some uncertain values could be obtained, but not for all species, and the values present higher uncertainty than usual (see Table 1). This may be attributed to the fact that only indirect spectrophotometric effect of the complex formation can be registered and in the mathematical evaluation, the ligand spectra recorded in the absence and presence of Ga(III) ion are fitted. Another problem is that only very low concentrations (3–$6 \times 10^{-5}$ M) can be used. Moreover, the hydrolysis of Ga(III) ion is quite favoured at such low concentrations, what can result in some error (the hydroxo species with their fixed stability constants [33] were involved into the equilibrium model, as detailed in the Section 2).

Representative examples for concentration distribution curves for the Fe(III) containing system are shown in Fig. 3.

### 3.4. Metal ion–IDAPipPr(3,4-HP)$_2$–Orn(3,4-HP) ternary system

Since one ligand molecule (IDAPipPr(3,4-HP)$_2$) can coordinate the studied three-charged metal ion *via* its two hydroxypyridinone chelating groups, saturation of the octahedral coordination sphere of these metal ions and formation of tris-chelated species can lead to the formation of polynuclear species. To obtain mononuclear

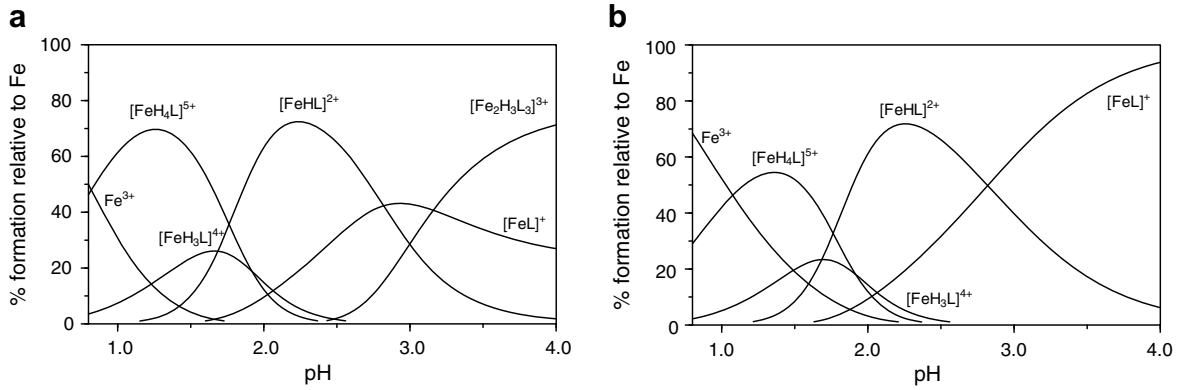


**Fig. 3.** Concentration distribution curves of the species formed in the system IDAPipPr(3,4-HP)$_2$/Fe(III) (a) (2:1) ligand to metal ration, $C_M = 2.21 \times 10^{-4}$ M, $C_L = 4.42 \times 10^{-4}$ M; and (b) (1:1) ligand to metal ratio, $C_L = 2.21 \times 10^{-4}$ M.

tris-hydroxypyridinonate complexes, a ternary systems was hypothesized, involving one metal ion, the bis-chelating IDAPipPr(3,4-HP)$_2$ and the mono-chelating Orn(3,4-HP).

The metal ion–Orn(3,4-HP) binary systems were previously studied [20] and the obtained species together with their stability constants were involved (as fixed values) into the equilibrium models of the ternary systems. All this data is presented in Table 1.

### 3.5. IDAPipPr(3,4-HP)$_2$ and Orn(3,4-HP) binary system

Following the characterization of the binary systems, the possibility of eventual ligand–ligand (IDAPipPr(3,4-HP)$_2$–Orn(3,4-HP)) interaction in solution was firstly evaluated. For that propose, three pH-potentiometric titration curves were performed at different $H_2L^1$:$HL^2$ molar ratios: (1:4), (1:2) and (1:1). The potentiometric curves could be well fitted including only the pre-determined $\log\beta$ values per each ligand. This suggests that, on the basis of the potentiometric measurements, no acid–base interaction between the two ligands could be detected. Spectrophotometric results are also in agreement with that feature (Fig. S4). In fact, if we consider the molar absorptivity of the two ligands at $\lambda_{max}$ 310 and 280 nm, take into account their concentrations and assume that there is no measurable interaction between them, "theoretical" absorbances for the binary $H_2L^1$–$HL^2$ system ($Abs_{theoretical}$) could be calculated. Comparison between experimental and theoretical values, obtained for the absorbance at 310 and 280 nm, the difference was only 0.022 and 0.020, respectively. This small difference could be accepted under the experimental error and we could conclude that both measurements (the spectrophotometry and the pH-potentiometric titrations) are in agreement and do not indicate any ligand–ligand (IDAPipPr(3,4-HP)$_2$–Orn(3,4-HP)) interactions. Also the simultaneous $^1$H NMR titration of both ligands in the same solution was in agreement with that finding, because the spectra was just the sum of the two individual $^1$H NMR spectra.

### 3.6. Metal ion–IDAPipPr(3,4-HP)$_2$–Orn(3,4-HP) ternary systems

To study the ternary system composed by both the ligands (IDAPipPr(3,4-HP)$_2$ ($H_2L^1$), Orn(3,4-HP) ($HL^2$)) and the $M^{3+}$ metal ions (M = Fe, Ga, Al), pH-potentiometric titrations were performed and, in case of Fe(III), a spectrophotometric titration at 1:1:1 stoichiometric ratio was also carried out. Noteworthy is the fact that the presence the ligand Orn(3,4-HP) in the ternary system resulted in a slight increase in the solubility of the complexes in aqueous solution, as compared with the binary metal–IDAPipPr(3,4-HP)$_2$ system. Thus, measurements at higher analytical concentrations became possible for the ternary systems with every metal ion. In fact, for this system, precipitation occurs only at pH around 9, whereas in the binary system it occurs below pH 2. As a consequence, spectrophotometric, and potentiometric measurements could be made. In these measurements, three different Metal:$H_2L^1$:$HL^2$ molar ratios were used (1:1:1, 1:1:2 and 2:1:4). Concerning the Fe(III) system, there was precipitation in the 1:1:1 potentiometric titration at around pH 7, whereas the other two titrations were performed without visible solubility problems. Therefore, to study the Fe(III):$H_2L^1$:$HL^2$ system, a spectrophotometric titration was also carried out at 1:1:1 molar ratio.

Analysis of the spectrophotometric spectra obtained for the IDAPipPr(3,4-HP)$_2$/Orn(3,4-HP)/Fe(III) system (Fig. 4) indicates that the monochelated complex starts to be formed at very low pH (at pH 1.0, $\lambda_{max}$ = 560 nm). With pH increase, the spectra is blue shifted, indicating the formation of the bis-chelated species ($\lambda_{max}$ = 510 nm), between pH 1.0 and 2.5. At pH around 2.5 the shift of the $\lambda_{max}$ from 510 to 460 nm starts, due to the formation of the tris-chelated species ($\lambda_{max}$ = 460 nm).

Both spectrophotometric and pH-potentiometric data were used to calculate the stability constants for the ternary complexes (Table 1). Based on these values, concentration distribution curves were also calculated and presented in Fig. 5. In this figure the $\lambda_{max}$ values as a function of pH are also represented. From the results, we can see that the complexation starts far below pH 1, and different species co-exist below pH 2.5–3. Although the bis-chelated species dominate at pH around 2, also the first ternary species, $FeH_3L^1L^2$, appears in measurable concentration. Most probably, the coordination mode in this species involves three hydroxypyridinonates moieties and the protons are expected to be at the amino group of $HL^2$, at the piperazine nitrogen and on the tertiary amine of $H_2L^1$. Almost parallel with this species, the formation of $FeH_2L^1L^2$ starts, becoming the predominated one by pH 4. Due to hydrolytic processes starting at pH ≅ 7, which seems to overlap the deprotonation process, the formation constants for the species $FeHL^1L^2$ and $FeL^1L^2$ can not be determined. Anyway, subtraction of the logarithmic values of the two stepwise deprotonation constants from the value calculated for the bis-protonated species (54.30 − 9.85 − 7.39 = 37.1; see Table 1) provides us a "theoretical value" for the $FeL^1L^2$ and this is in agreement with those generally obtain for a tris-hydroxypyridinonate Fe(III) complex [20,39].

In the case of Al(III), the formation of the tris-chelated species started at higher pH than in case of iron (pH around 3), which means that the first species to be formed is $AlH_2L^1L^2$, because the tertiary amine is already deprotonated.

Noteworthy is the fact that the results obtained for the calculated formation constants with those of the model ligands, namely for the tris-chelated species formed with 3,4-DMHP and M(III) (see

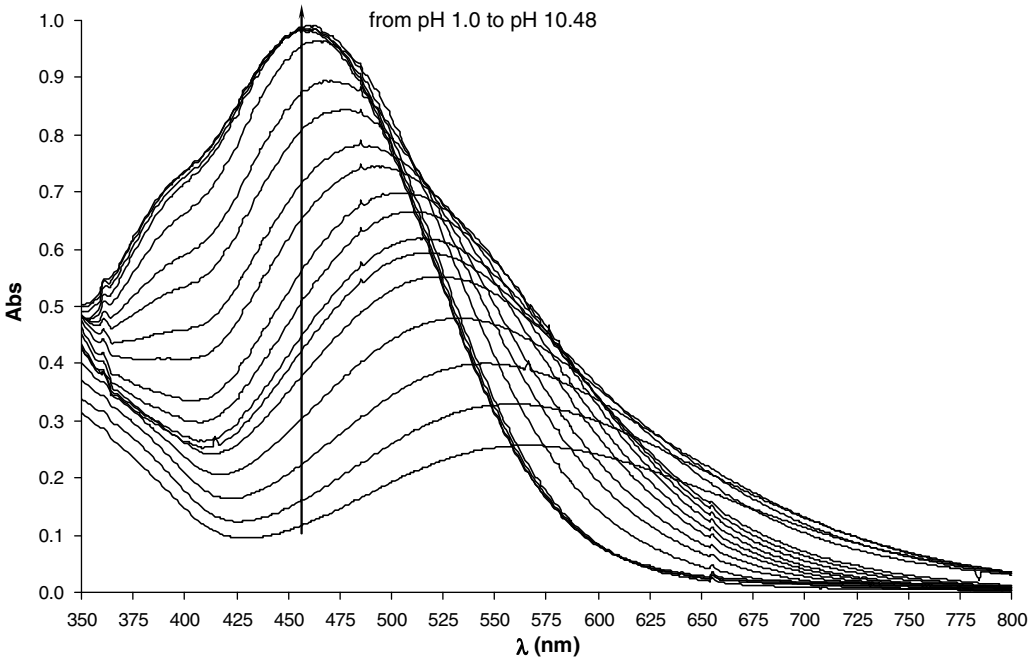


**Fig. 4.** Absorption spectra for the IDAPipPr(3,4-HP)$_2$/Orn(3,4-HP)/Fe(III) system registered at various pH values at: $C_{Fe} = 2.01 \times 10^{-4}$ M, $C_{H2L1} = 2.06 \times 10^{-4}$ M and $C_{HL2} = 2.10 \times 10^{-5}$ M. $T = 25.0$ °C. $I = 0.2$ M KCl.

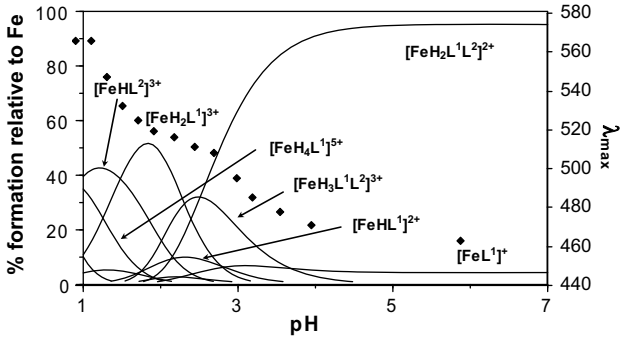


**Fig. 5.** Concentration distribution curves of the species formed in the system IDAPipPr(3,4-HP)$_2$/Orn(3,4-HP)/Fe(III) at (1:1:1) ligand to metal ration, $C_M = C_{H2L1} = C_{HL2} = 1.0 \times 10^{-5}$ M, and pH dependence of $\lambda_{max}$ of UV–Vis spectra (♦).

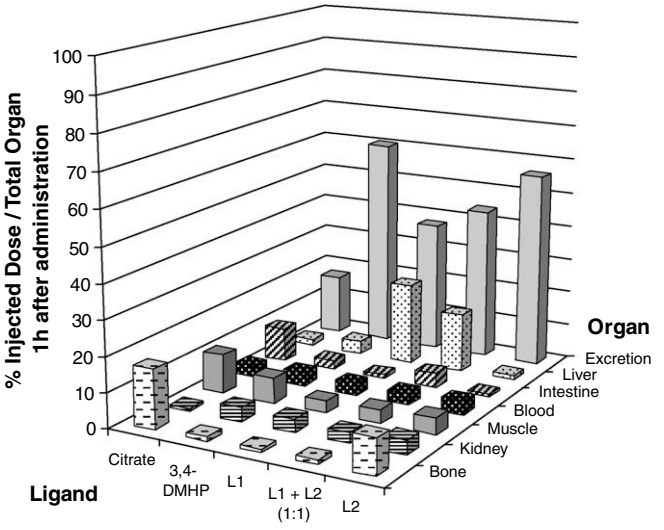


**Fig. 6.** Biodistribution data in percent of injected dose per total organ of $^{67}$Ga-citrate and $^{67}$Ga-citrate with simultaneous intraperitoneal injection of 3,4-DMHP, IDAPipPr(3,4-HP)$_2$ ($L^1$), Orn(3,4-HP) ($L^2$), and a 1:1 mixture of IDAPipPr(3,4-HP)$_2$/Orn(3,4-HP), 1 h after intravenous administration in mice.

Table 1), are in very good agreement with those expected for the coordination of three hydroxypyridinone groups to the $Al^{3+}$ metal ion.

For the Ga(III) system, only titrations with the higher excess of $HL^2$ relative to $H_2L^1$ (1:0.5:2) showed no precipitation. For the other two stoichiometric conditions, the precipitation occurs at pH around 3. However, since there are no actual results for the formation constants of the $H_2L^1$/Ga(III) complexes, no reasonable fit of the data could be obtained for the ternary system.

Anyway, comparison the pH-potentiometric titrations for the ternary systems with all three metal ions, suggest the same coordination mode. The bis- and tris-chelated species are formed, in case of Fe(III) and Ga(III) at lower pH than in case of Al(III) (pH 2 instead of pH 3).

For comparison between the metal (M) chelating efficacy of the ligands in study with those of some others with biological interest, the corresponding pM values at the diluted conditions that prevail in biological systems (pM = $-\log[M^{3+}]$ for pH 7.4, at micromolar concentration of the metal ion and 10-fold ligand excess) reported in the literature are also depicted in Table 1. The bis-hydroxypyridinone containing systems showed higher affinity than other currently used drugs for metal decorporation (DFP or 3,4-DMHP) or for delivering $^{68}$Ga for diagnostic purposes (DOTA or DTPA) [40], but somewhat lower affinity than that of deferrioxamine [4,41].

### 3.7. Biodistribution assays

To assess the effect of using a combination of these tetra- and bis-dentate 3,4-HP ligands ($H_2L^1$ and $HL^2$) for the metal decorporation and eventual coadjuvation effects, solutions containing these ligands were administered to mice which had been previously injected with $^{67}$Ga-citrate. This animal model was selected due to the known similarities between gallium and the target metal ions (Al,

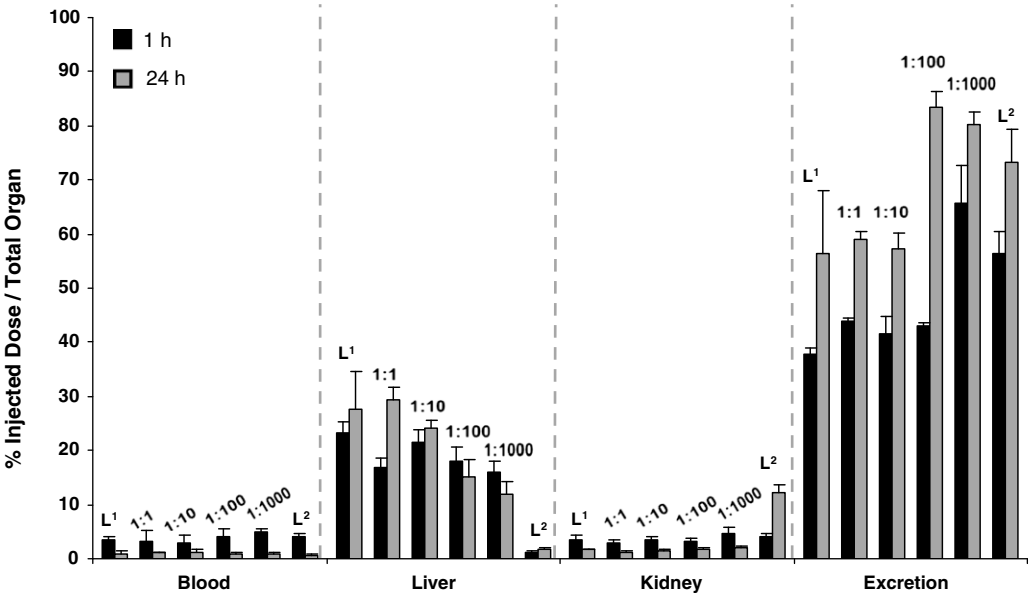


**Fig. 7.** Biodistribution data in percent of injected dose per total organ of $^{67}$Ga-citrate and $^{67}$Ga-citrate with simultaneous intraperitoneal injection of the ligands: IDAPipPr(3,4-HP)$_2$ ($L^1$), Orn(3,4-HP) ($L^2$) and IDAPipPr(3,4-HP)$_2$/Orn(3,4-HP) at indicated ratio, at 1 h and 24 h after intravenous administration on mice.

Fe), namely in terms of physico-chemical properties and binding interactions with 3,4-HPs and biological ligands [20,45], as well as to the easy assessment of the metal content in the different organs.

On a first assay, after administration of the radiotracer, three groups of animals were respectively injected with $H_2L^1$ and $HL^2$ and mixture of both ligands at 1:1 molar ratio. After 1 h administration of the ligands, tissue distribution of the $^{67}$Ga was assessed for the main organs of each group of animals, as well as for a separated group of control $^{67}$Ga-injected animals. The metal biodistribution values are presented as percent of injected dose per total organ in Fig. 6, together with the corresponding values previously reported for 3,4-DMHP and $HL^2$ [17].

These bioassays clearly demonstrate the ability of the chelating agents to complex *in vivo* and to eliminate the metal ion. In fact, the radioactivity clearance from most organs and the rate of excretion from whole animal body are enhanced, as compared to those of $^{67}$Ga-citrate. A comparative analysis of biodistribution data from the chelating agent $H_2L^1$, administered alone or combined with $HL^2$, shows an improved profile of the combined system, namely on the excretion rate and the decrease of the liver uptake. The relatively rapid total excretion suggests the urinary tract as the main excretory route although a significant fraction of radioactivity seems to be also eliminated by hepatobiliar pathway, as indicated by the liver and intestines radioactivity accumulation.

The combined chelation was further explored *in vivo* with $H_2L^1$ and $HL^2$ at different dose proportions. The results of whole body excretion and biodistribution on main organs are shown in Fig. 7, for each dosage molar ratio. The use of different $H_2L^1$:$HL^2$ ratios was undertaken to clarify the effect related to the combined use of the two ligands.

The fastest excretion rates are obtained with administration of chelator combination cocktails, namely for the $H_2L^1$/$HL^2$ molar ratios (1:100 and 1:1000). This may be understood in terms of thermodynamics requirements for some competition between the two chelators for the metal ion, to enable effective coadjuvation and synergistic effects due to their complementary accessibility to different sites and organs. The radioactivity uptake in main organs, such as liver and kidneys, presents considerable dose-percentage dependence and suggests the coexistence of both excretion pathways, urinary and hepatobiliar.

The mechanism involved in the $^{67}$Ga-citrate accumulation on disease site or normal tissue is not clearly known, although it has been accepted that, as a Fe analogue, $^{67}$Ga can bind to serum proteins, mostly transferrin (Tf) [46,47], and access to cells, eventually through a Tf receptor, although the mediation of other proteins is also admitted [42,48]. However, the gallium affinity for $HL^2$ (pGa = 20.6) [20] and Tf (pGa = 20.3) [42] are very close, thus supporting the existence of some eventual competition, an important feature for chelation therapy.

From these studies we can conclude that, for the stoichiometric conditions used in the combined system, there might be some coadjuvating effect associated to the use of the mixture of two chelating agents with different physico-chemical properties (chelating affinity, molecular weight, partition coefficient).

## 4. Conclusions

The chelating properties of a new bifunctional bis-hydroxypyridinone towards three-charged *hard* metal ions (Fe, Al, Ga) have been evaluated in solution and *in vivo*, alone or in combination with a mono-hydroxypyridinone ligand, to explore potential coadjuvating effects that could benefit the metal decorporation. The complexation studies with the ternary system indicates the same metal affinity but improvements on the solubility of the metal complexes, as compared with the binary bischelating system, an important feature for the metal complex excretion, upon sequestration. This might be due to the absence of polynuclear species associated with M(III)-bis-hydroxypyridinone complexes but also to the higher hydrophilicity of the amino-acid moiety of the mono-hydroxypyridinone. The bis-hydroxypyridinone containing systems showed somewhat lower affinity than that of deferrioxamine but higher than other currently used drugs for metal decorporation (e.g. DFP) or for delivering of $^{68}$Ga for diagnostic purposes (e.g. DOTA, DTPA). The results of the *in vivo* studies with $^{67}$Ga injected mice show differences on the biodistribution profiles of the radiotracer, upon the administration of each chelating agent or their combination, which might be ascribed to an improved accessibility of the ligands to different cellular compartments.

From these studies one can conclude that, for the stoichiometric conditions used in the combined system, there might be some coadjuvating/synergic effect associated to the use of the mixture of the two chelating agents, namely when a big excess of the mono- over the bis-chelator is used.

## Acknowledgments

The authors thank to the Portuguese Fundação para a Ciência e Tecnologia (FCT) (Project PDCT/QUI/56985/2004; Ph.D. Grant SFRH/BD/8743/02), to the Hungarian Scientific Research Fund (OTKA T049612) and Portuguese-Hungarian bilateral program and COST D21/001 for financial support. The authors are also grateful to Dr. Guilhermina Cantinho from Instituto de Medicina Nuclear of Medical University of Lisbon for the kind support given to the bioassays.

## Appendix A. Supplementary material

Potentiometric titration curves of IDAPipPr(3,4-HP)$_2$ alone and in the presence of Al(III); absorption spectra for the IDAPipPr(3,4-HP)$_2$/Fe(III) system registered at various pH values; absorbance in the UV region, at indicated pH values for the free ligand, and for the IDAPipPr(3,4-HP)$_2$/Ga(III) system; absorbance in the UV region, at indicated pH values, for the system IDAPipPr(3,4-HP)$_2$/Orn(3,4-HP).

Supplementary data associated with this article can be found, in the online version, at doi:10.1016/j.jinorgbio.2008.10.020.

## References

[1] N.C. Andrews, New Eng. J. Med. 341 (1999) 1986–1995.
[2] G. Crisponi, M. Remelli, Coord. Chem. Rev. 252 (2008) 1225–1240.
[3] T. Kiss, K. Gajda-Schrantz, P. Zatta, in: A. Sigel, H. Sigel, R.K.O. Sigel (Eds.), Metal Ions and Life Sciences, Neurodegenerative Diseases and Metal Ions, Wiley & Sons, Chichester, 2006, pp. 371–393.
[4] Z.D. Liu, R.C. Hider, Coord. Chem. Rev. 232 (2002) 151–171.
[5] D.Y. Liu, Z.D. Liu, R.C. Hider, Best Pract. Res. Clin. Haematol. 15 (2002) 369–384.
[6] A.L. Florence, A. Gauthier, R.J. Ward, R.R. Crichton, Neurodegeneration 4 (1995) 449–455.
[7] B. Wonke, C. Wright, A.V. Holffbrand, Br. J. Haematol. 103 (1998) 361–364.
[8] G.J. Kontoghiorghes, Hemoglobin 30 (2006) 329–347.
[9] G.J. Kontoghiorghes, Curr. Med. Chem. 12 (2005) 2661–2662.
[10] A. Kattamis, Ann. N. Y. Acad. Sci. 1054 (2005) 175–182.
[11] J.L. Esparza, M. Gómez, J.L. Domingo, D. Del Castillo, M. Hernandez, Pharmacol. Toxicol. 87 (2000) 33–38.
[12] T.P. Kruck, J.G. Cui, M.E. Percy, W.J. Lukiw, Cell. Mol. Neurobiol. 24 (2004) 443–459.
[13] C.J. Anderson, M.J. Welch, Chem. Rev. 99 (1999) 2219–2234.
[14] K.H. Thompson, C.A. Barta, C. Orvig, Chem. Soc. Rev. 35 (2006) 545–556.
[15] M.A. Santos, Coord. Chem. Rev. 228 (2002) 187–203.
[16] R. Grazina, L. Gano, J. Sebestik, M. A. Santos, J. Inorg. Biochem. (2008) in press.
[17] M.A. Santos, S. Gama, L. Gano, G. Cantinho, E. Farkas, Dalton Trans. 21 (2004) 3772–3781.
[18] S. Piyamongkol, T. Zhou, Z.D. Liu, H.H. Khodr, R.C. Hider, Tetrahedron Lett. 46 (2005) 1333–1336.
[19] M.A. Santos, M. Gil, S. Marques, L. Gano, G. Cantinho, S. Chaves, J. Inorg. Biochem. 92 (2002) 43–54.
[20] M.A. Santos, M. Gil, L. Gano, S. Chaves, J. Biol. Inorg. Chem. 10 (2005) 564–580.
[21] D.E. Green, C.L. Ferreira, R.V. Stick, B.O. Patrick, M.J. Adam, C. Orvig, Bioconj. Chem. 16 (2005) 1597–1609.
[22] M.A. Santos, Coord. Chem. Rev. 252 (2008) 1213–1224.
[23] G.L. Patrick, An Introduction to Medicinal Chemistry, Oxford University Press Inc., New York, 2004.
[24] B.R. De Costa, L. Radesca, L. Di Paolo, W.D. Bowen, J. Med. Chem. 35 (1992) 28–47.
[25] B.R. De Costa, X. He, J.T.M. Linders, C. Dominguez, Z.Q. Gu, W. Williams, W.D. Bowen, J. Med. Chem. 36 (1993) 2311–2320.
[26] C.S. John, B.J. Vilner, B.C. Geyer, T. Moody, W.D. Bowen, Cancer Res. 59 (1999) 4578–4583.
[27] W.L.F. Armarego, D.D. Perrin, Purification of Laboratory Chemicals, Butterworth Heinemann Press, Oxford, 1999.
[28] G. Gran, Acta Chem. Scan. 4 (1950) 559–577.
[29] M.A. Santos, S.M. Marques, A. Rossello, T. Tuccinardi, P. Carelli, L. Panelli, Bioorg. Med. Chem. 14 (2006) 7539–7550.
[30] H.M. Irving, M.G. Miles, L.D. Pettit, Anal. Chim. Acta 38 (1967) 475–488.
[31] C.F. Baes, R.E. Mesmer, The Hydrolysis of Cations, Wiley, New York, 1976.
[32] E. Farkas, E. Kozma, T. Kiss, I. Toth, B. Kurzak, J. Chem. Soc. Dalton Trans. (1995) 477–481.
[33] L.O. Ohman, W. Forsling, Acta Chem. Scan. Ser. A – Phys. Inorg. Chem. 35 (1981) 795–802.
[34] L. Zékány, I. Nagypál, Computational Methods for the Determination of Stability Constants, Plenum Press, New York, 1985.
[35] A. Leo, C. Hansch, D. Elkins, Chem. Rev. 71 (1971) 525–616.
[36] P.K. Glasoe, F.A. Long, J. Phys. Chem. 64 (1960) 188–190.
[37] P. Gans, A. Sabatini, A. Vacca, J. Chem. Soc. Dalton Trans. (1985) 1195–1200.
[38] E.T. Clarke, A.E. Martell, Inorg. Chim. Acta 191 (1992) 57–63.
[39] E.T. Clarke, A.E. Martell, Inorg. Chim. Acta 196 (1992) 185–194.
[40] A.E. Martell, R.M. Smith, R.J. Motekaitis, Critically Selected Stability Constants of Metal Complexes Database, College Station TX, Version 4, 1997.
[41] E. Farkas, E.A. Enyedy, H. Csoka, Polyhedron 18 (1999) 2391–2398.
[42] R.J. Motekaitis, Y. Sun, A.E. Martell, Inorg. Chim. Acta 159 (1989) 29–39.
[43] R.J. Motekaitis, A.E. Martell, Inorg. Chim. Acta 183 (1991) 71–80.
[44] S. Chaves, M. Gil, S. Marques, L. Gano, M.A. Santos, J. Inorg. Biochem. 97 (2003) 161–172.
[45] M.A. Santos, R. Grazina, A.Q. Neto, G. Cantinho, L. Gano, L. Patrício, J. Inorg. Biochem. 97 (2000) 303–311.
[46] S.W. Gunasekera, L.J. King, P.J. Lavender, Clin. Chim. Acta 39 (1972) 401–406.
[47] S.M. Larson, J.S. Rasey, D.R. Allen, Z. Grunbaum, J. Nucl. Med. 20 (1979) 843–846.
[48] T. Hara, Int. J. Nucl. Med. Biol. 1 (1974) 152–154.